

Abstract

Post-service destructive evaluation was performed on two commercially pure zirconium pump impellers. One impeller failed after short service in an aqueous hydrochloric acid environment. Its exposed surfaces are bright and shiny, covered with pockmarks, and peppered with pitting. Uniform corrosion is evident and two deep linear defects are present on impeller blade tips. In contrast, the undamaged impeller surfaces are covered with a dark oxide film. This and many other impellers in seemingly identical service conditions survive long lives with little or no apparent damage.

No material or manufacturing defects were found to explain the different service performance of the two impellers. Microstructure, microhardness and material chemistry are consistent with the specified material. Examination reveals the damage mechanism to be corrosion-enhanced cavitation erosion, the most severe form of erosion corrosion. Cavitation damage to the protective oxide film caused the zirconium to lose its normally outstanding corrosion resistance.



Figure 1 – View of the damaged zirconium impeller. Several sections have been removed for evaluation. Note the linear defects (arrows). (0.2X)

The root cause of the impeller failure is most likely the introduction of excessive air into the pump due to low liquid level, a bad seal or inadequate head. Corrosion pitting, crevice corrosion and solidification cracks (casting defect) also contributed to the failure.

Introduction

Remnants of two zirconium impellers were submitted to IMR Test Labs (a division of Ithaca Materials Research) for post-service materials analysis. Both impellers were utilized in chemical industry circulation pump applications in the Mid-East. Analysis of the aqueous acidic pumpage reveals 50 g/L HCl, 3 g/L MgCl₂, 3 g/L CaCl₂, and 10-50 ppm Br₂.

The impeller shown in Figure 1 failed after only three months of service. Gross degradation was discovered upon pump disassembly. The second impeller (Figure 2) survived twelve years of service without significant deterioration. The purpose of this materials evaluation was to determine the cause of the impeller damage.



Figure 2 – View of the undamaged impeller. Portions have been removed for evaluation. Its surfaces are covered with a dark, protective oxide film. (0.2X)

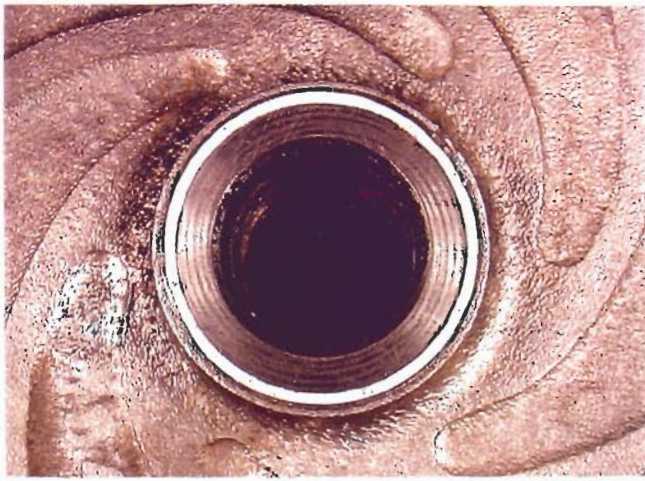


Figure 3 – Pock marks due to cavitation exhibit a flow pattern in the vicinity of the central hub. (0.7X)



Figure 4 – Patches of corrosion pitting are evident on the damaged impeller surface. (1.1X)

Failure Analysis

Visual Examination

The undamaged impeller surfaces are uniformly covered with a dark oxide film. This is typical of zirconium, which owes its superior corrosion resistance in oxygen-containing environments to the spontaneous formation of an adherent protective oxide film. Furthermore, the impeller surfaces are relatively smooth and free of obvious corrosion pitting or other attack.

In contrast, the exposed surfaces of the damaged impeller are very clean, shiny and covered with pock marks. Material loss is evident. This appearance is consistent with cavitation damage, the degradation of a metal surface due to the hammer-like blows created by the formation and rapid collapse of vapor bubbles within a liquid undergoing severe turbulent flow. Vapor bubbles form when the local pressure is reduced below the vapor pressure and implode as they pass into a region of higher pressure. Collapse pressures are extremely high and can cause loss of material, surface damage, and/or changes in properties/appearance. For the case of a zirconium impeller, cavitation erosion, the most severe form of erosion-corrosion, is a concern. Cavitation erosion is the accelerated attack caused by the synergistic effects of: (1) cavitation damage to the metal surface and protective oxide film; (2) erosion due to relative motion between the metal surface and the liquid; and (3) corrosion of the exposed base metal.

Figure 3 shows the surface appearance of the damaged impeller in the vicinity of the hub. The pock marks due to cavitation exhibit a flow pattern. This texture is consistent with cavitation erosion and not typical of an as-cast surface. In addition to the pock-marked surface, the damaged impeller is peppered with corrosion pitting. The worst area of pitting is shown in Figure 4. Zirconium and zirconium alloys are extremely resistant to corrosives, including the aqueous

hydrochloric acid (HCl) service environment experienced by the subject impellers. Only a few environmental species will attack zirconium. These include hydrofluoric acid (HF), ferric chloride (FeCl_3), cupric chloride (CuCl_2) and moist chlorine gas. Assuming that cavitation occurred in the aqueous HCl service environment, it is reasonable to expect detrimental chlorine gas to be present in the vapor bubbles.

Figure 5 presents two of the three obvious linear defects present on the impeller blades. The defects are open-mouthed and the surface appearance within the defects is pock-marked like the outer surfaces of the impeller.

Metallography

Metallographical cross sections of the impellers were prepared to investigate the apparent corrosion pitting, to examine material



Figure 5 – A closer view of two deep linear defects on an impeller blade tip. (1.2X)



Figure 6 – Photomicrograph showing a cross section of a corrosion pit. (50X)

microstructure, and to accommodate micro-hardness measurements. The samples were etched with 45 ml H₂O, 45 ml HNO₃, 5 ml HF and 90 ml lactic acid for approximately 5 seconds. Figures 6 and 7 present metallographic cross sections through two areas of pitting. The subsurface tunneling appearance of the attack (Figure 6) is consistent with corrosion pitting. The maximum observed pit depth is ~0.8 mm.

Figure 8 shows the microstructure typical of the damaged and undamaged impellers. Both display Widmanstätten structure (basket weave appearance) typical of zirconium and most of its alloys in the unannealed condition. Upon cooling, zirconium undergoes an allotropic transformation at approximately 870°C (1600°F) from a body-centered cubic crystal structure (β phase) stable at high temperatures to a hexagonal close-packed crystal structure (α phase) stable at low temperatures. This transformation generally results in a Widmanstätten structure of

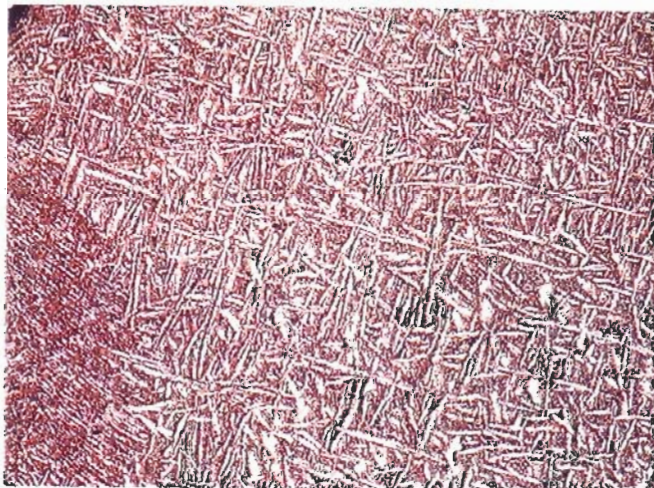


Figure 8 – Both impellers display a Widmanstätten structure. (100X)

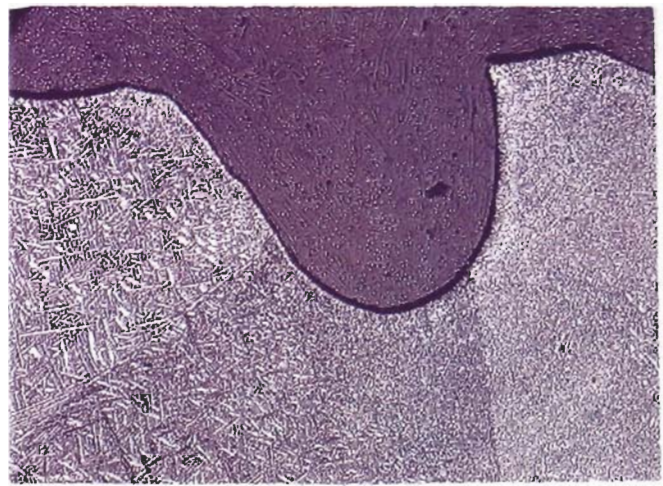


Figure 7 – Metallographic cross section through another corrosion pit. (50X)

α -zirconium. The more rapid the cooling rate, the finer the Widmanstätten structure.¹

Fractography

One of the linear defects observed on the impeller blades was sectioned and parted to permit fractographic evaluation. The fracture surface (Figure 9) consists of three distinct regions: (1) the defect mouth which resembles the pock-marked impeller surface; (2) a tight crack-like area covered with a black deposit; and (3) the fresh fracture created in the laboratory to part the defect for examination. Apparently, the defects started as tight cracks and then opened up under the influence of crevice corrosion and cavitation. Crevice corrosion occurs by a similar mechanism as pitting and is due to the development of a corrosive environment (e.g., buildup of detrimental species) inside the stagnant crevice.

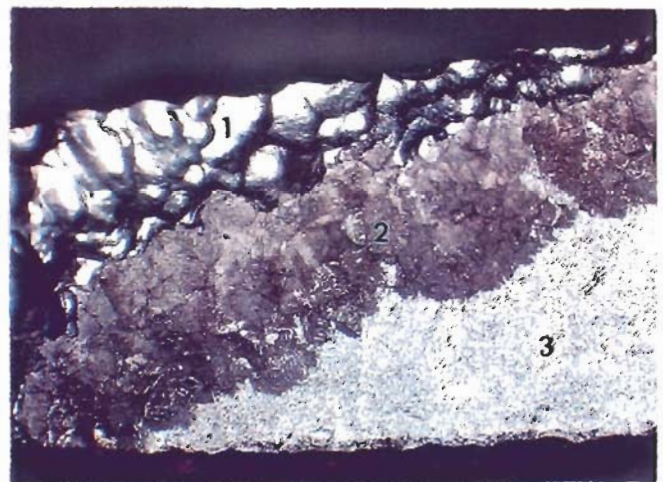


Figure 9 – The linear defect fracture surface exhibits three distinct regions. (8.8X)



Figure 10 – Closer view of the solidification crack fracture surface. Note the Widmanstätten structure. (24X)

A closer view of the dark portion of the fracture surface reveals the Widmanstätten structure (Figure 10). This fracture morphology suggests that the cracks formed during solidification of the casting. The site of these defects, the ends of the blades where material thickness varies rapidly, is also consistent with solidification cracking.

Chemistry

The material chemistries of the damaged and undamaged impellers were analyzed using ASTM Standard Methods C 1111-88 and E 1019-94 (modified: steel calibration standards). The results are shown in Table 1. Both impellers conform to the specification for commercially pure zirconium (Grade 702, UNS R60702). Carbon and nitrogen, two elements known to be potentially detrimental to the corrosion performance of zirconium are actually present in higher concentrations in the undamaged impeller. It is noted that the corrosion resistance of commercially pure zirconium in aqueous environments is highly variable.

Table 1 – Impeller Chemical Compositions

Element	Damaged Impeller	Undamaged Impeller	UNS R60702
Hf	0.45	0.02	4.5 max.
Fe	0.09	0.10	---
N ¹	0.014	0.017	0.025 max.
C ¹	0.018	0.027	0.05 max.
O ¹	0.19	0.16	---
Other	<0.5	<0.5	<0.8
Zr	Balance	Balance	Balance

¹ Determined by combustion.

Energy dispersive spectroscopy (EDS) was employed for chemical analysis of the fracture surface of one of the linear defects on the damaged impeller blades. Figure 11 presents the EDS spectrum for the black deposit on the tight crack-like

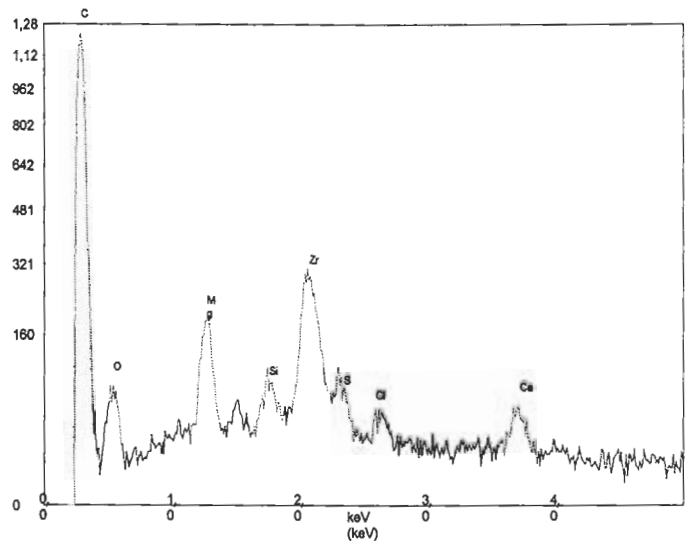


Figure 11 – EDS chemical analysis of the black deposit within a linear defect reveals high carbon from the graphite casting mold.

portion of the defect. This region is rich in carbon, attributed to graphite mold material used in casting the impeller. This contaminated surface layer may have adversely affected corrosion resistance. Also noteworthy is the iron-rich debris found in the open-mouth portion of the defect (Figure 12). Iron, if present as ferric chloride (FeCl_3), could account for accelerated corrosion rates. The presence of Fe^{3+} polarizes the zirconium surface to a potential exceeding the pitting potential, which leads to localized breakdown of the protective passive film and corrosion pitting.²

Micro-Hardness

The hardness of the two impellers was determined per ASTM E 384. The average measured hardness of the damaged and undamaged impellers is 186 and 209 $\text{HK}_{500\text{g}}$, respectively. These minor hardness differences do not account for the observed performance differences.

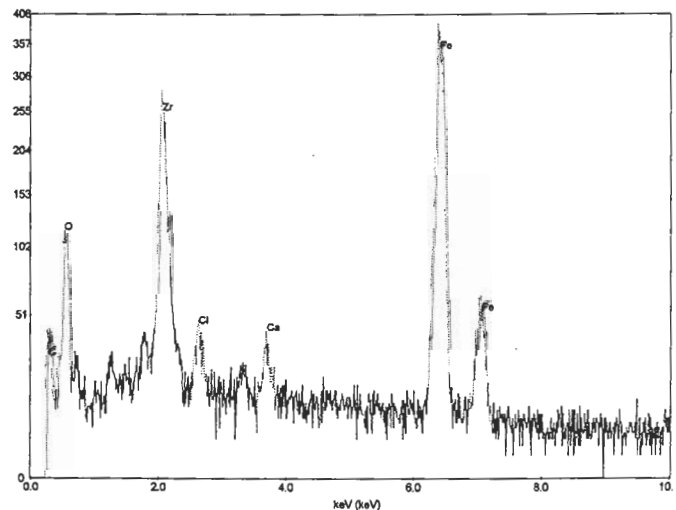


Figure 12 – EDS chemical analysis reveals iron-rich debris in the open-mouth portion of a linear defect.

Summary and Conclusions

1. The impeller damage mechanism is cavitation erosion. Possible causes are a turbulent flow pattern caused by the impeller motion, excessive air (e.g., low liquid level in supply tank or introduction of air through a pump seal), or inadequate head.
2. Pitting corrosion, crevice corrosion and, most importantly, corrosion-enhanced cavitation erosion contributed to the impeller failure. In addition to the aqueous hydrochloric acid environment, chlorine gas and ferric chloride are potential corrosive agents.
3. Solidification cracks (casting defects) on blade tips served as preferred sites for deep cavitation erosion.

Acknowledgements

The author gratefully acknowledges the contributions of Dave Christie and Steve Ruoff of IMR Test labs, and Jack Tosdale of Oremet-Wah Chang. Dave gathered background information, initiated the failure analysis, and provided valuable technical input. Steve overviewed the entire effort, reviewed this paper, and recommended excellent editorial changes. Jack performed independent failure analysis and shared his expertise on zirconium alloys.

References

1. T.L. Yau and R.T. Webster, "Corrosion of Zirconium and Hafnium", *Metals Handbook*, 9th Edition, Volume 13, 707-721 (1987)
2. R. T. Webster, "Zirconium and Hafnium", *Metals Handbook*, 10th Edition, Volume 2, 661-669 (1990)